NUMERICAL SIMULATION OF EARTHQUAKES AND TSUNAMIS IN MEXICO – Case Study: Earthquake and Tsunami of 8 September 2018

Raissa Mazova [1,2], Sergey Tyuntyayev [3], Adel Giniyatullin[1], Yury Orlov[1], Evgeny Orlov[1], Vladimir Mel'nikov[1]

[1]*Nizhny Novgorod State Technical University n.a. R.E. Alekseev, 603600 Nizhny Novgorod, Russian Federation*
[2]*Moscow Institute of Physics and Technology (MIPT) 141701 Moscow, Russian Federation ,e-mail:* raissamazova@yandex.ru
[3]*Harman Connected Services (HCS), Nizhny Novgorod, Russian Federation; e-mail:* ser.tyuntyaev@gmail.com

 ABSTRACT

The present study pertains to a catastrophic earthquake with a magnitude of M = 8.1, which occurred in the southern region of Mexico on September 8, 2018. Taking into account the location of the earthquake source and its hypocenter, a numerical simulation of the generation of a seismic source of tsunami waves and their propagation over the water area for two different mechanisms of the seismic source, with their different localizations, was carried out. Two-block and four-block earthquake sources are considered and the obtained wave characteristics are compared with field data and data of other authors.

Keywords: *source of earthquake, tsunami waves, numerical modeling.*

1. INTRODUCTION

As predicted earlier by a number of authors (see, e.g., [1]), seismic activity along the perimeter of the Pacific Ocean should increase significantly by the end of the 20th and the beginning of the 21st centuries. The appearance of large earthquakes and associated tsunamis in the Pacific and Indian Oceans, at the beginning of this century, supports this assumption. The importance of this assumption leads to the need for a deeper analysis of historical data on catastrophic tsunamigenic earthquakes in specific ocean regions in order to reduce the tsunami hazard for coastal areas.
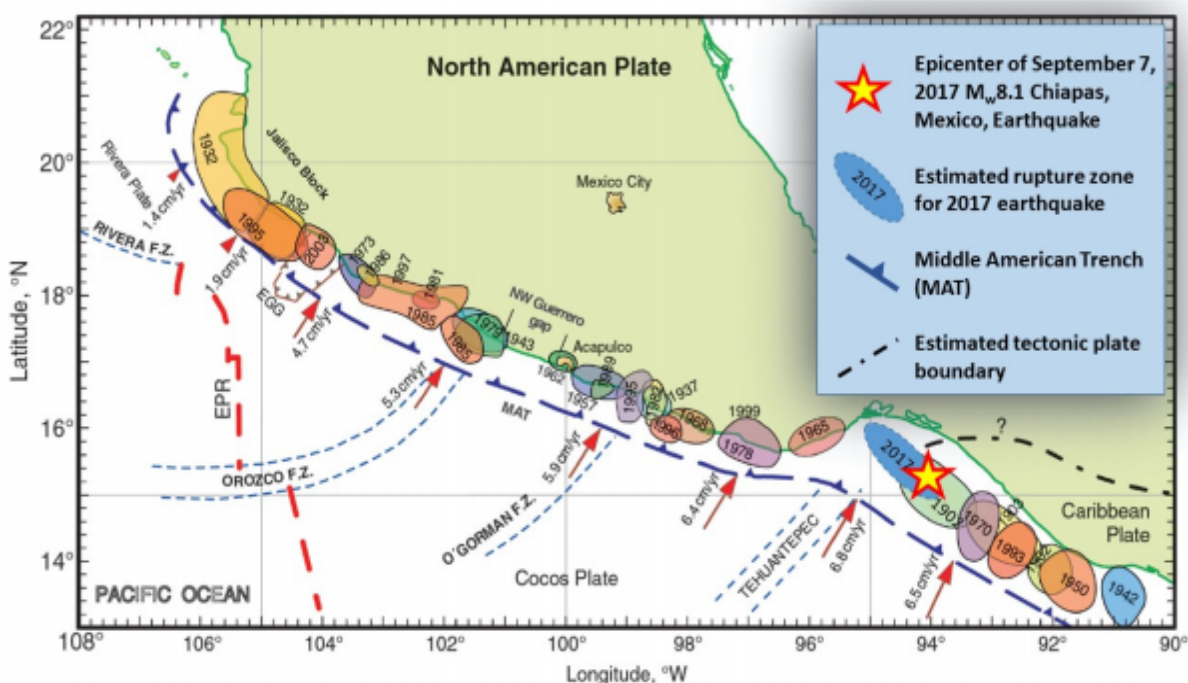

Fig.1. Historic Earthquakes in the Pacific Coastal Region of Mexico [2-3]

For example, it is well known that some of the largest earthquakes that occurred on the Guerrero coast (see Fig. 1), and located parallel to the active Mexican subduction zone, generated tsunamis. The occurrence of such historic earthquakes and tsunamis in this region has been relatively well documented since the 16th century. For example, during the last century, large earthquakes occurred near the Pacific coast of Mexico, such as in Jalisco in 1932 (M = 8.2), in Colima in 1995 (M = 8.0), and the earthquake in Mihoatskune in 1985 (M = 8.1), which devastated the coast of Mexico City, resulting in large human and economic losses, estimated in billions of dollars. Nevertheless, information about the geological evidence of earthquakes and a detailed description of the tsunami caused by them is practically not documented [2].

2. THE 8 SEPTEMBER 2017 EARTHQUAKE IN MEXICO

At the location of this event, the Cocos Plate converges with the North American Plate (see Fig. 2) at a rate of approximately 76 mm / yr, in a northeasterly direction. The Cocos Plate begins its subduction in Central America, 100 km southwest of this earthquake. Location, depth and mechanism of formation of faults of this earthquake indicates that the event is intraplate [3,4]. This earthquake is one of the largest ever recorded on the southern coast of Mexico. The tsunami wave following the earthquake caused significant damage and dozens of deaths. In the state of Oaxaco 45 people died, in the state of Chiapas 12 people and in the state of Tabasco 4 people, schools and hospitals were also de-energized. [5]
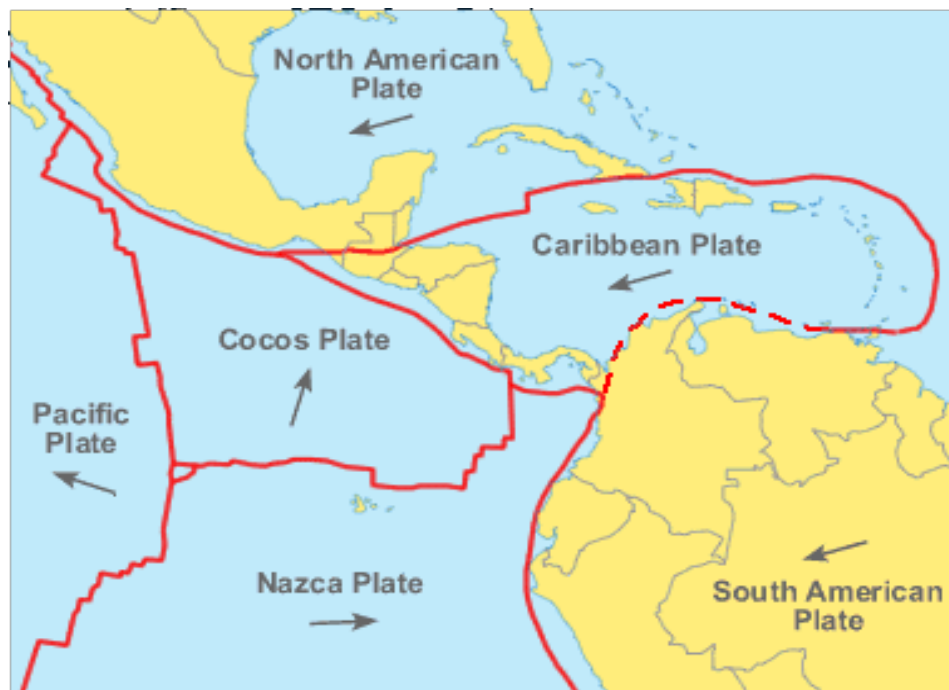

Fig. 2. The fault pattern (red lines) in the region of Central America. Black arrows indicate the direction of movement of the continental plates [5, 15]

3. STATEMENT OF THE PROBLEM

The location of the source for the numerical simulation of the considered earthquake was chosen based on the location of the hypocenter and processing of data from the NEIC information center [4, 5, 15, 16]. In Fig.3, the position of the seismic source on the map is shown, where the localization of aftershocks is marked with black dots.
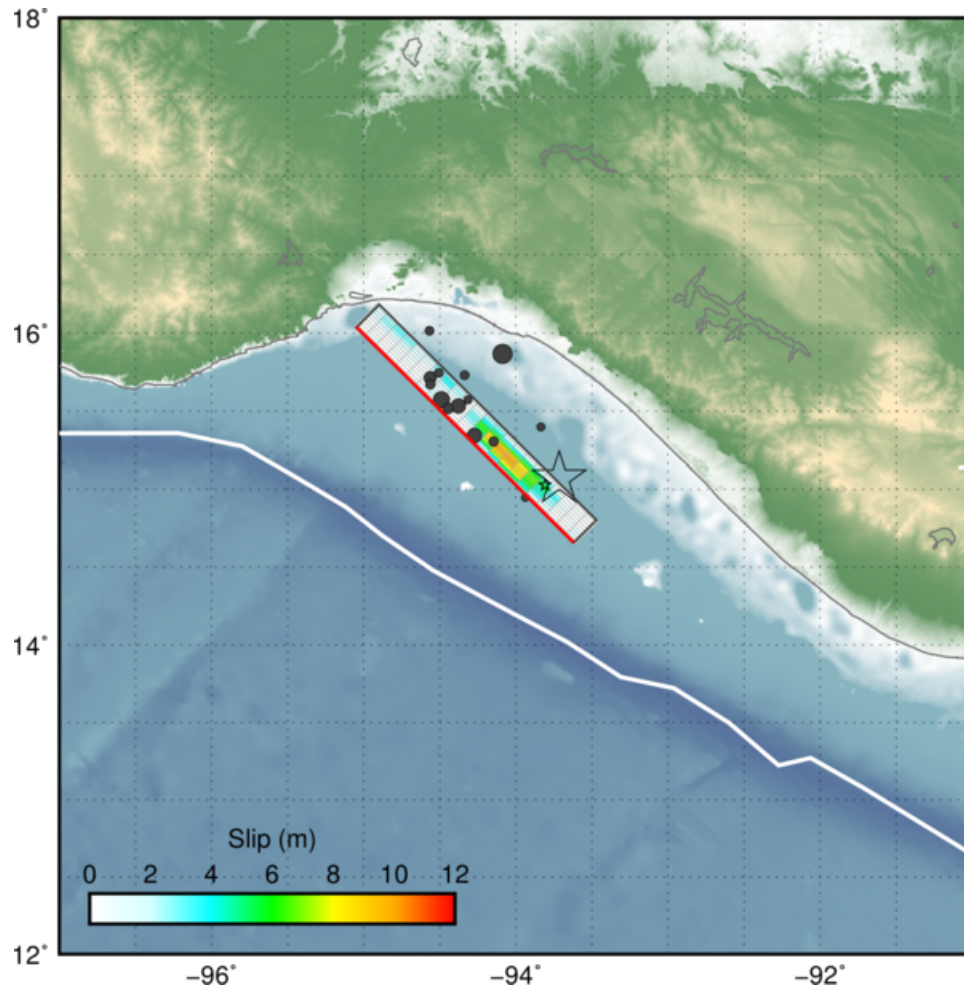
Fig. 3. Position of the seismic source on the map. The black dots mark the location of aftershocks [4]

Using the data given in [4, 5, 15, 16] and the results of [2-3], on the basis of the keyblock model of the earthquake source [6, 9], two possible scenarios for the realization of the Earth's crust movements in the region of the seismic source for this earthquake were considered:

In the first Scenario, a two-block source is considered, divided lengthwise into two longitudinal blocks. The implementation of the movement of blocks in the seismic source occurs in 35 seconds (Table 1). The first block, oriented towards the shore, moves down 3 meters within 20 seconds, the second block, oriented towards the open ocean, it rises 6 meters in 20 seconds, and its movement begins 15 seconds later than the movement of the first block. Fig.4 shows the location of the seismic source on the bathymetric map.

For the second Scenario, a kinematic model of a seismic source consisting of four blocks was used. The division into blocks during the selection of the seismic source was carried out according to the intensity and location of aftershocks (Fig.3, Fig.5). The implementation of the movement of blocks in the seismic source occurs in 30 seconds (Table 1).
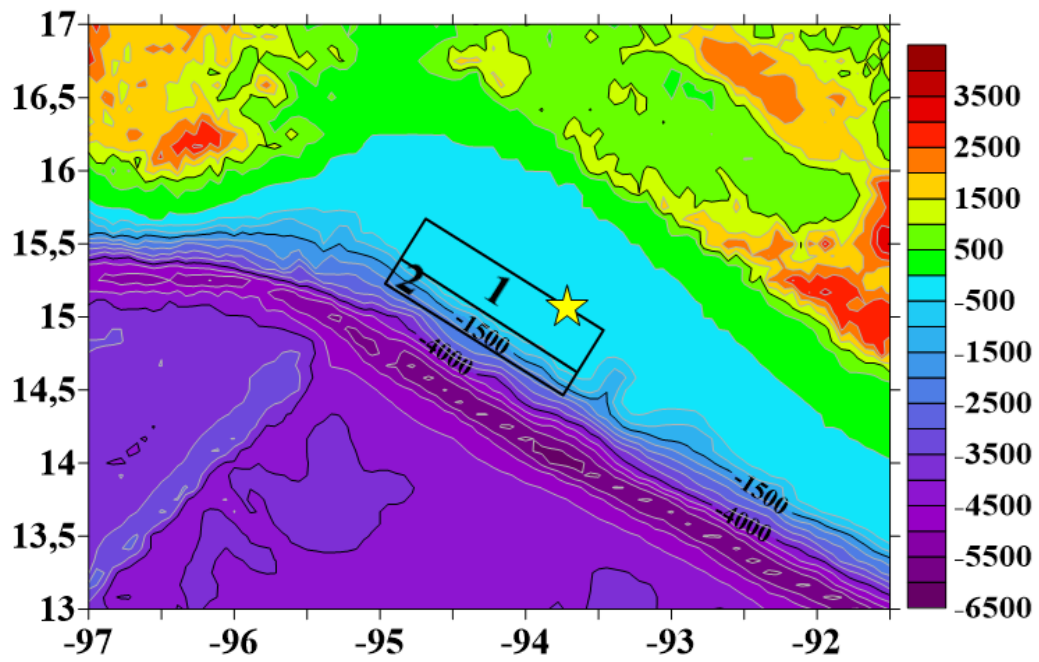
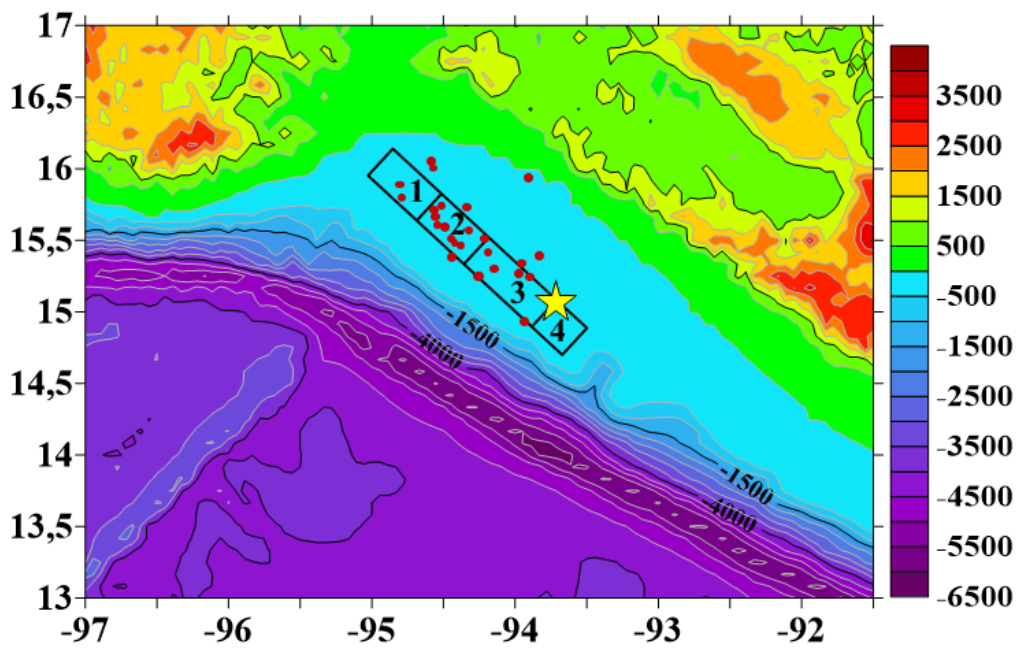Fig. 4 Position of seismic source on Bathymetric map for Scenario 1.

Fig. 5. Position of seismic source on bathymetric map for Scenario 2

The considered movements of the key blocks in the earthquake source for these two possible scenarios are given in Table 1.

Table 1. The movement of blocks in the earthquake source for Scenario 1 and 2

	Scenario 1		Scenario 2			
	Block №					
	1	2	1	2	3	4
Start of uplift (s)	0	15	10	5	0	10
Time of uplift (s)	20	20	10	15	20	10
Height of uplift (m)	-3	6	-0.5	2	6	0.5

4. MATHEMATICAL STATEMENT OF THE PROBLEM.

In this paper, we study long surface waves with lengths and periods characteristic of tsunamis. The non-linear system of shallow water equations [7-11] is used to describe the process of wave generation and propagation in accordance with the assumptions that were mentioned above.

$$\begin{cases} \vec{U}_t + \vec{U} \cdot grad\ \vec{U} + g \cdot grad\eta = 0 \\ \eta_t + div\left((H + \eta - B)\vec{U}\right) = B_t \end{cases} \qquad \vec{U} = \begin{pmatrix} u \\ v \end{pmatrix} \tag{1}$$

Here the functions u and v are the velocities of water particles; g - acceleration due to gravity, $B(x,y,t)$ - function describing the law of motion of the bottom of the basinl; for a keyboard model, the function $B(x,y,t)$ describes the sequential movement of the key blocks.

The mechanism of realization of the movements of the Earth's crust in the seismic source was given from tectonic considerations using the WELLS formulas [12].

$$\lg L = 0{,}59M - 2{,}44 \pm 0{,}16$$

$$\lg W = 0{,}32M - 1{,}01 \pm 0{,}15 \qquad , \tag{2}$$

where M is the magnitude of the earthquake; L is the length of the rupture in the source (in km), W is the width of the rupture plane (in km). For this earthquake source, the parameters obtained are as follows: the source length will be 233 ± 82, and the source width will be 40 ± 14.

Using the Iida formula (3) (see, e.g., [8]), for a given earthquake with a magnitude of $M = 8.1$, the vertical component of the displacement of the water surface above the earthquake source can be obtained using the formula

$$\lg(H/2) = 0{,}8M - 5{,}6 \tag{3}$$

where M is the magnitude of the earthquake, and H is the maximum height of the vertical displacement of the bottom at the source of the earthquake. The values obtained by formulas (1) and (2) were used to simulate the generation of the tsunami source in scenarios 1 and 2.

Scenario 1. Let us consider the results of numerical simulation of scenario 1. For Scenario 1, an earthquake source is selected, consisting of two blocks, located along the coastline, and the block oriented towards the coast (block 1) has a negative shift (see Table 1). The entire process of tsunami source generation (water displacement on the surface of the water area above the earthquake source) during the movement of blocks takes 35 s. Fig.6 shows three time moments during the generation of the tsunami source. By the corresponding displacement of the wave surface, one can determine the downward movement of the first block (Fig. 6, left panel), then at 20 s, the rise of the second block by approximately 1.4 m (Fig. 6, middle panel) and at the 35th s the generation of the tsunami source ended (Fig.6, right panel).
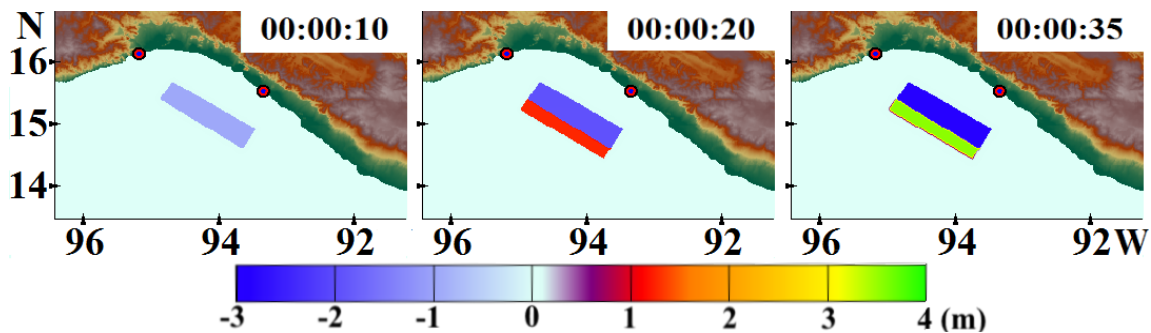

Fig. 6. Generation of the tsunami source for Scenario 1: a) 10s; b) 20 s; c) 35 s.

In Fig. 7 the position of the wave fronts when implemented in the considered water area is presented. It is clearly seen that at 23 min (Fig. 7, upper left panel), the elevation waves with a height of 0.2-0.5 m approach the cities of Mexico, Salina Cruz and Puerto Escondido. At the 33rd min (Fig.7, upper right panel), both points have already attacked by the first wave, and also the eastern front with an elevation with a height of 0.1-0.3 m approaches the city of Champerico (Guatemala). With a further spread to 48 minutes (Fig. 7, lower left panel), the western front continues to cover the southeast of Mexico, approaching the city of Acapulco with a height of up to 0.2 m, and the eastern front reaches El Salvador with a height of up to 0.1 m, namely to the city of Akahutla. After 1 hour and 20 min (Fig.7, lower left panel), the waves reached all near-field points, and also approach the cities of Lazaro Cardenas and Tamarindo with heights of up to 0.1 m.
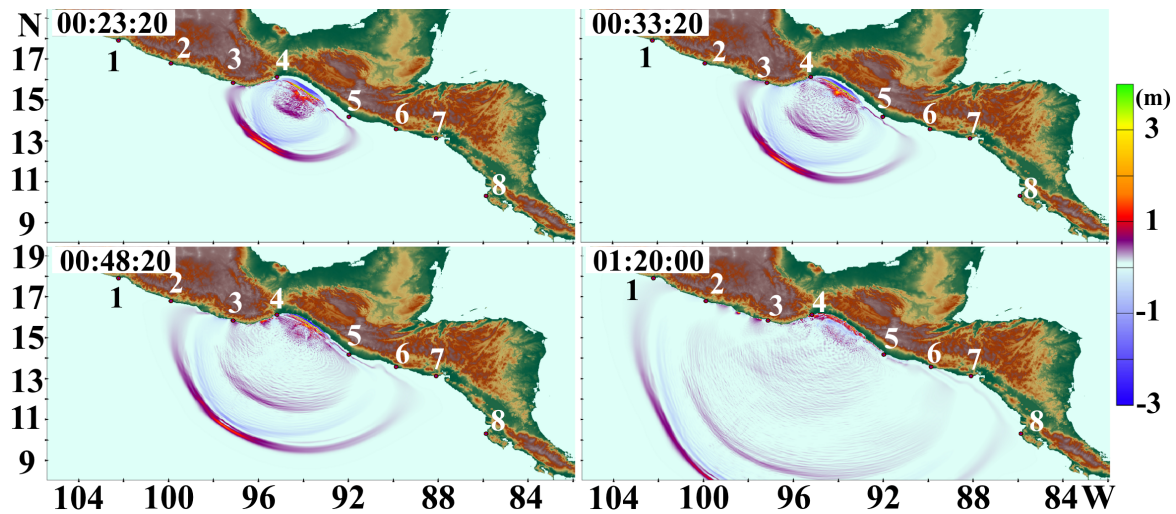
Fig.7. Position of wave fronts in numerical simulation for Scenario 1 for 4 time points: 1. Lazaro Cardenas (Mexico); 2. Acapulco (Mexico); 3. Puerto Escondido (Mexico); 4. Salina Cruz (Mexico); 5. Champerico (Guatemala); 6. Acajutla (Salvador); 7. El Cuco (Salvador); 8. Tamarindo (Costa Rica)

In Fig.8, the maximum distribution of wave heights over the entire calculated area is presented. The distribution of the maximum wave heights clearly shows that the most dangerous areas are near-field points, namely the cities: Salina Cruz (Mexico), (item 4), Puerto Escondido (Mexico), (item 3) and Champerico (Guatemala), (p.5).
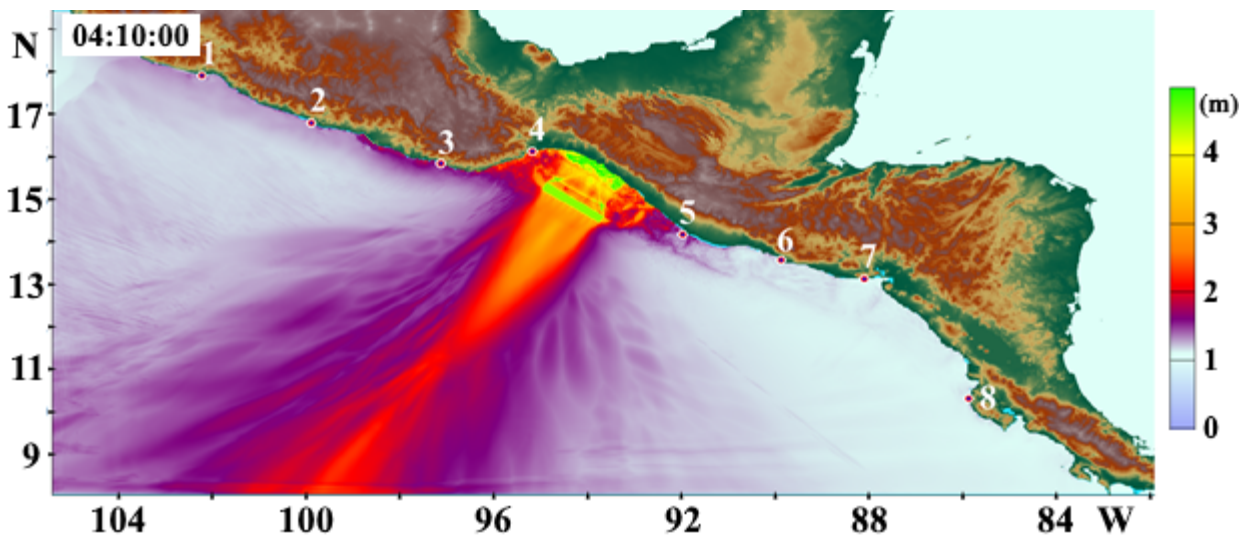

Fig. 8. The distribution of maximum wave heights in the water area when implementing Scenario 1: 1. Lazaro Cardenas (Mexico); 2. Acapulco (Mexico); 3. Puerto Escondido (Mexico); 4. Salina Cruz (Mexico); 5. Champerico (Guatemala); 6. Acajutla (Salvador); 7. El Cuco (Salvador); 8. Tamarindo (Costa Rica).

A more detailed distribution of the maximum tsunami wave heights along the coasts can be seen on the 3D histograms of the maximum wave heights plotted on the 5-meter isobath shown in Fig. 9. It is clearly seen that on the Mexican coast near the cities of Puerto Escondido and Acapulco (Fig.9a), the wave heights change in the region from 0.1 to 1 m. You can also notice that the most dangerous coast is the south the eastern coast of Mexico near the city of Salina Cruz (Fig. 9c), where the maximum wave height reaches 1.5 m. On the coast of Guatemala (Fig. 9b), the maximum wave height reaches 1.3 m, and in the area of the city of Champerico, the heights vary from 0.1 to 0.3 m.
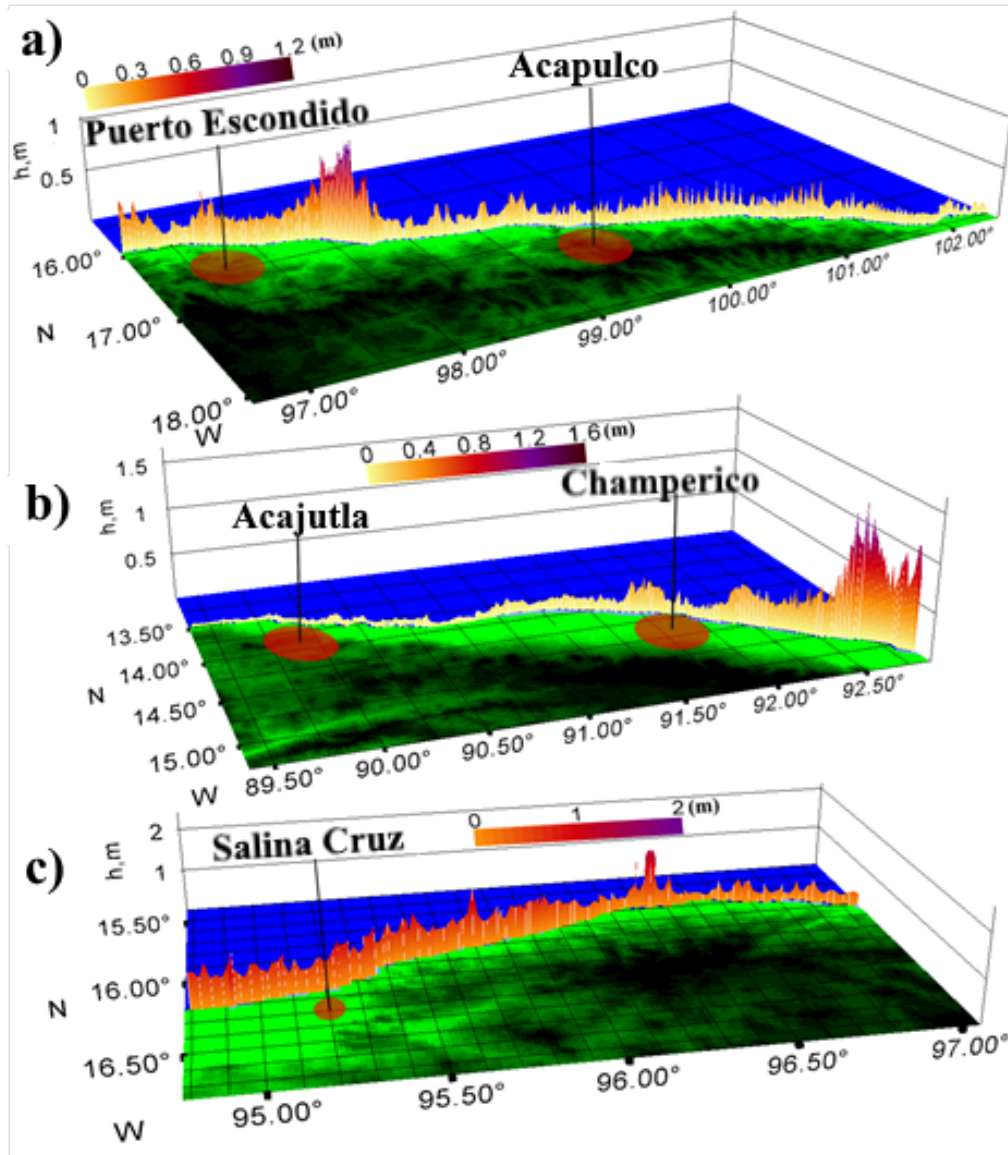

Fig. 9. Two-dimensional histograms for maximum wave heights on a 5-meter isobath when implementing scenario 1: a) Mexico; b) Guatemala, El Salvador; c) Salina Cruz (Mexico)

But the coast of El Salvador near the city of Akahutla is less dangerous compared to neighboring Guatemala, and the maximum wave heights reach up to 0.1. Data from virtual tide gauges, namely the maximum wave height, the largest decrease in the water level and the time of wave arrival to points, are given in Table 2.

Table 2. Data of virtual tide gauges for Scenario 1.

City name	Maximum wave height at 5m isobath (m)	Strongest water level depression at 5m isobath m)	Time of approaching the point
01. Lazaro Cardenas (Mexico)	0.24	-0.29	01:22:55
02. Acapulco (Mexico)	0.3	-0.3	00:52:55
03. Puerto Escondido (Mexico)	0.51	-0.96	00:25:00
04. Salina Cruz (Mexico)	1.35	-1.8	00:01:15
05. Champerico (Guatemala)	0.39	-0.36	00:38:45
06. Acajutla (Salvador)	0.24	-0.38	01:11:15
07. El Cuco (Salvador)	0.15	-0.14	01:42:55
08. Tamarindo (Costa Rica)	0.19	-0.26	01:26:15

5. RESULTS OF NUMERICAL SIMULATION FOR SCENARIO 2

The division into blocks during the implementation of the scenario under consideration was carried out according to the intensity and location of aftershocks (see Fig. 3, 5). Fig. 5 shows the position of the seismic source on the bathymetric map, divided into 4 blocks. The movement of the source starts from the 3rd block to a height of 6m in 20 s, then 10 s after the start of the rise of block 3, block 2 begins to move up to a height of 3m for 15 s. Blocks 1 and 4 begin to move up from 15 s within 10 s to a height of 1 m (see Table 1). Figure 10 shows the generation of a tsunami source for scenario 2, when blocks move in the earthquake source shown in Table 1.
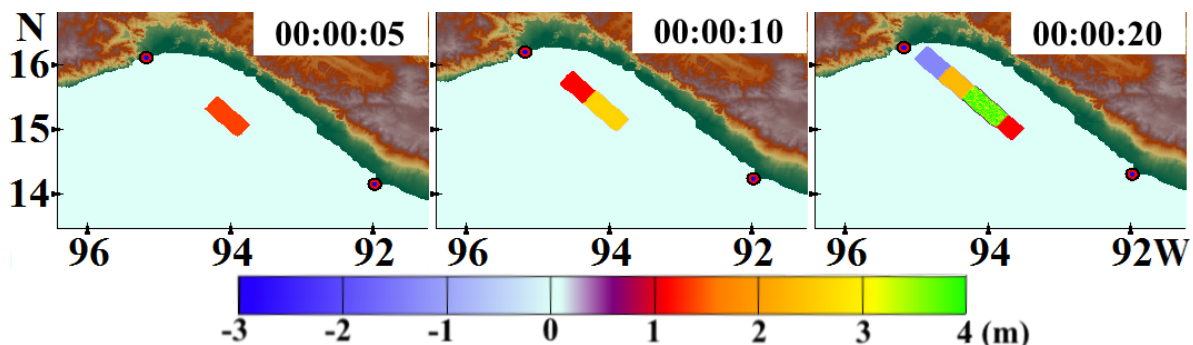

Fig. 10. Generation of the tsunami source in the implementation of Scenario 2

In Fig. 11 the position of the wave fronts in the numerical simulation of scenario 2 is presented. On the upper left panel, it is seen that the depression wave is approaching the city of Salina Cruz. Further, by the 35th min (Fig.11 (2)), the wave has already reached Salina Cruz, the western front with elevation approaches the Puerto Escondido and the eastern front approaches the coast of Guatemala. At the 55th min (Fig.11 (3)), the wave with elevation approaches Champerico Guatemala). With further propagation (1h 50m), the western front continues to cover the coast of Mexico, and is coming to the city of Acapulco, and the eastern front approaches the city of Akahutla (Fig. 11 (4)). After 1 hour 35 min from the beginning of the calculation (Fig.11 (5)), the wave covered most of the computed water area, so in the west, the wave reaches the city of Lazaro Cardenas, and in the east it approaches the cities of Tamarindo (Costa Rica) and El Cuco (Salvador). By 2h 2min (Fig. (11.6)), the wave covered the entire computed area.
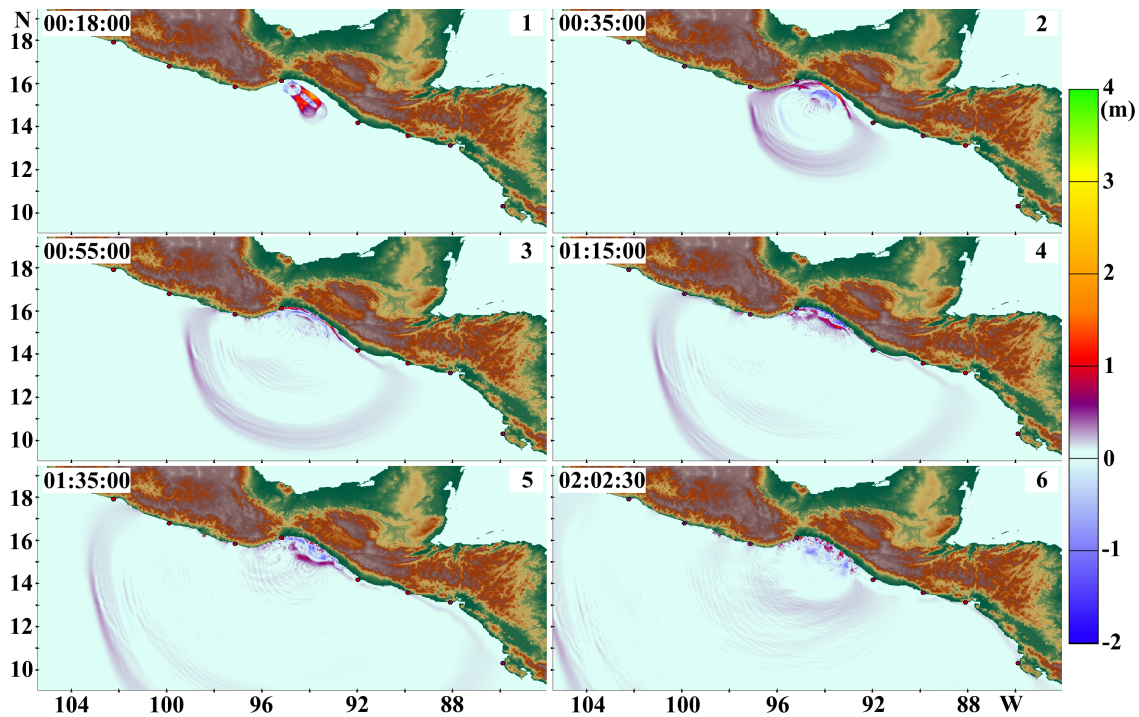

Fig. 11. Position of wave fronts in the numerical simulation of Scenario 2 for 6 time moments

Figure 12 shows the maximum distribution of wave heights. The distribution shows that the most dangerous areas are the cities: Salina Cruz (Mexico, p.4), Puerto Escondido (Mexico, p.3) and Champerico (Guatemalla, p.5).
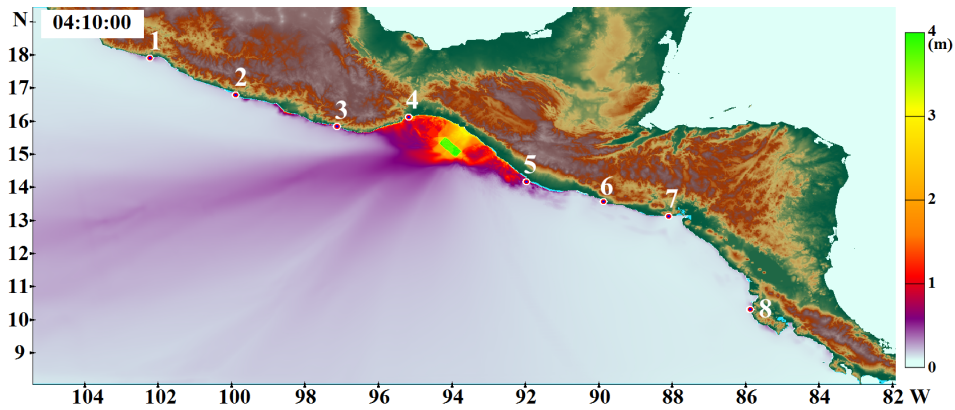
Fig. 12. The distribution of the maximum wave heights in the water area in the implementation of Scenario 2

A more detailed distribution of the maximum wave heights along a number of Pacific coasts can be seen in Fig.13, which shows two-dimensional histograms of the distribution of the maximum wave heights on the 5-meter isobath.
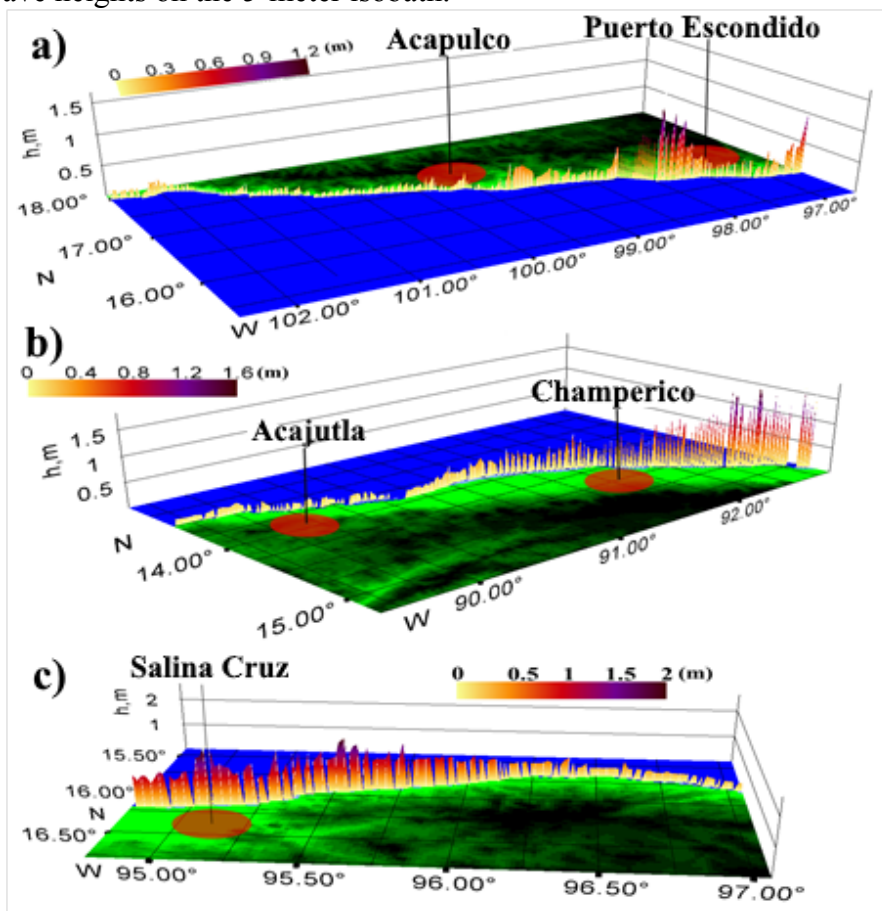

Fig. 13. Two-dimensional histograms for maximum wave heights on a 5-meter isobath in the implementation of Scenario 2 for the coasts: a) The coast of Mexico; b) The coast of Guatemala and El Salvador; c) Coast of Mexico near the city of Salina Cruz

It is clearly seen that on the coast of Mexico near the city of Acapulco the maximum wave height does not exceed 0.3 m, and on the coast near the city of Puerto Escondido the maximum wave height varies from 0.3 to 1 m (see. Fig.13 (a)). The maximum wave heights along the Guatemala and Salvador coasts (fig.13 (b)) decrease from west to east. Thus, the maximum wave heights near the coast of Champerico (Guatemala) vary from 0.2 to 1.5 meters, and near the coast of Acajutla (Salvador) they reach 0.2m. The highest wave heights are reached near the coast of the earthquake located near the source, so near the coast of Salina Cruz (Mexico), (Fig. 13 (c)) the maximum wave heights vary from 0.3 to 2 meters.

Data from virtual tide gauges, namely, the maximum wave height, the greatest decrease in the water level and the time of wave arrival to points, can be seen in Table 3.

Table. 3. Data from virtual tide gauges obtained during Scenario 2 implementation.

City name	Maximum wave heights at 5m isobath (m)	Strongest water level depression at 5m isobath (m)	Time of approaching the point
01. Lazaro Cardenas (Mexico)	0.25	-0.19	00:36:15
02. Acapulco (Mexico)	0.16	-0.08	00:19:10
03. Puerto Escondido (Mexico)	0.48	-0.5	00:04:10
04. Salina Cruz (Mexico)	1.38	-1.58	00:00:50
05. Champerico (Guatemala)	0.34	-0.4	00:46:15
06. Acajutla (Salvador)	0.26	-0.3	01:19:10
07. El Cuco (Salvador)	0.09	-0.1	01:51:40
08. Tamarindo (Costa Rica)	0.09	-0.1	01:34:35

6. COMPARISON OF NUMERICAL SIMULATION RESULTS

Table 4 shows comparisons of the data obtained with the results given in [13, 14, 15, 16,] for the earthquake under consideration. It should be noted that for the earthquake under consideration, data are provided only at some points along the coast. In a number of points given in [13, 14, 15, 16], where we also had virtual tide gauges are displayed, we have the possibility to compare the computation data. These data are shown in Table 3.

Table 4. Comparison of computation results with real data and date of another authors

Maximum wave heights / Название пункта	Scenario 1	Scenario 2	[15]	[16]	Real data [13]	Real data [14]
01. Lazaro Cardenas (Mexico)	0.24	0.25	-	0.3	0.219	0.25
02. Acapulco (Mexico)	0.3	0.16	-	-	-	0.7
03. Puerto Escondido (Mexico)	0.59	0.48	-	-	-	-
04 Salina Cruz (Mexico)	1.35	1.38	1.8	2.1	1.33	1.2
05. Champerico (Guatemala)	0.39	0.34	-	-	-	-

06. Acajutla (Salvador)	0.24	0.26	0.1	0.18	0.194	0.13
07. El Cuco (Salvador)	0.15	0.09	-	-	-	-
08. Tamarindo (Costa Rica)	0.19	0.09	-	-	-	-

It can be seen that the results of our computations are in better agreement with real data than, e.g., with works [15, 16].

Figures 14 and 15 also show a comparison of the tide gauges of both scenarios with data taken from real sensors for the city of Salina Cruz (Mexico). For scenario 1 (Fig. 14) it can be seen that the time of income of a positive wave, as well as the maximum tendency of the behavior of the wave propagating from the earthquake source, remains to be unchanged.
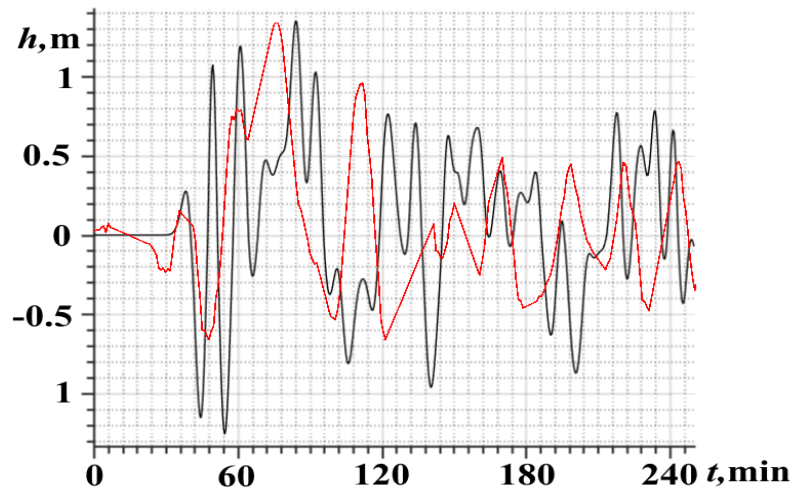

Fig. 14. Comparison of tide-gauge records of scenario 1 with real data for the city of Salina Cruz (Mexico)
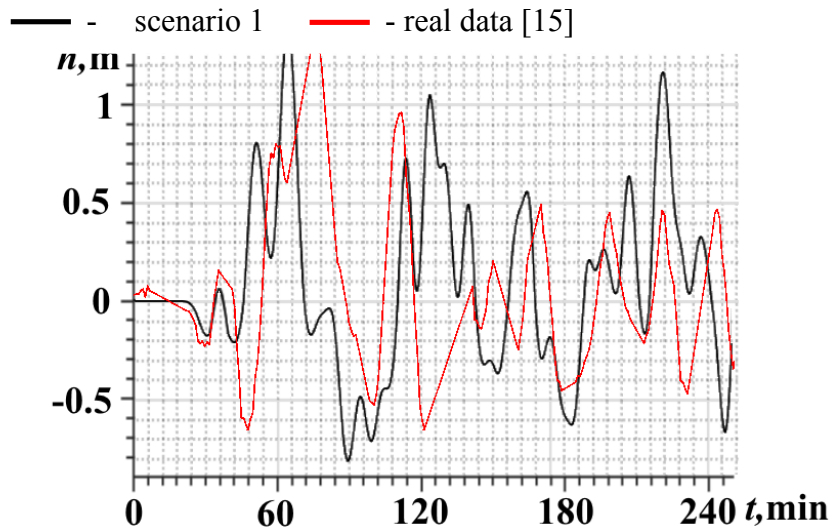

Fig. 15. Comparison of tide-gauge records of scenario 2 with real data for the city of Salina Cruz (Mexico).

Comparing scenario 2 with real data (Fig.15), it can be seen that in both cases the negative wave is the first to approach, and the maximum and minimum tendencies of the wave's behavior also remains to be unchanged.

Figures 16-19 show histograms for comparing the results of computations carried out in this work with the results of works [13, 14]. It is clearly seen that all scenarios are in good agreement with real data, with the exception of the point located in the area of 100 ° W (Acapulco city). The maximum heights do not exceed 3.8 m, both in our computations and in the histograms from [13, 14]. When comparing scenario 1 with work [13] (Fig. 16) and with work [14] (Fig. 17), it can be seen that the distribution of the maximum wave heights are similar, but in the region of 94 ° -96 ° W. there are differences. The maximum distribution of waves obtained in the implementation of scenario 2 has a distribution pattern that is closer to the works [13, 14] than the maximum distribution of scenario 1 (see Figs.17, 19).
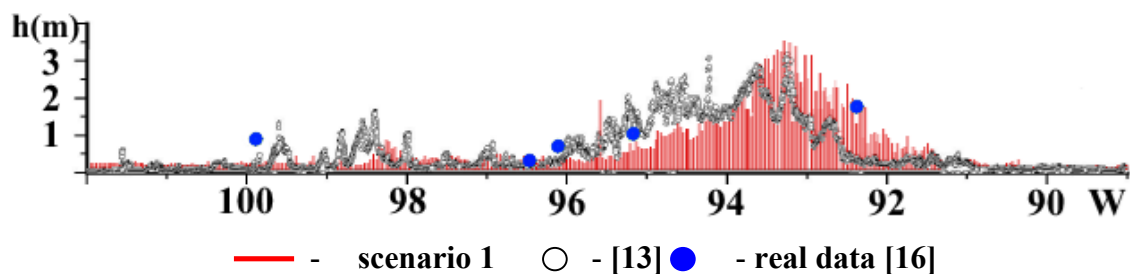

Fig. 16. Comparison of the histograms of the distribution of the maximum wave heights of scenario 1 with the work [13] for the calculated coast
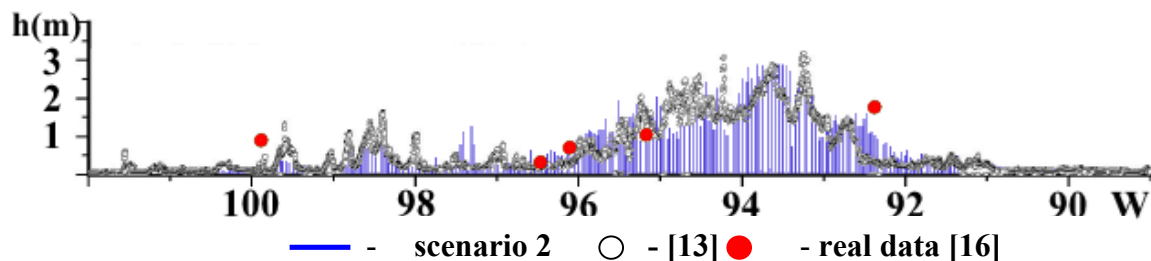

Fig. 17. Comparison of the histograms of the distribution of the maximum wave heights of scenario 2 with the work [13] for the calculated coast
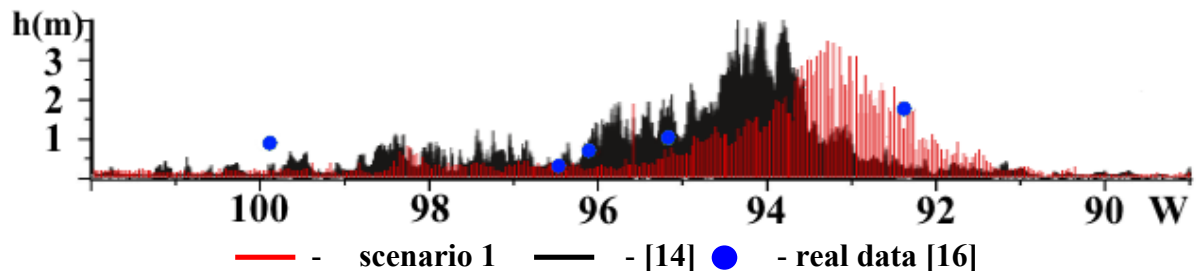

Fig. 18. Comparison of the histograms of the distribution of the maximum wave heights of scenario 1 with the work [14] for the calculated coast
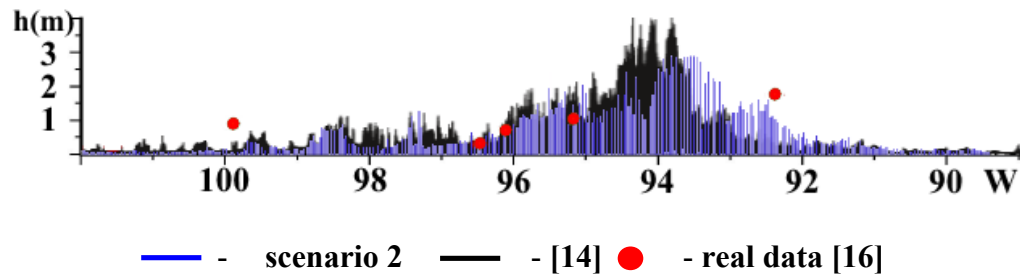
Fig. 19. Comparison of the histograms of the distribution of the maximum wave heights of scenario 1 with the work [14] for the calculated coast.

Thus, the analysis of the maximum wave heights for the selected 8 points of the water area in numerical modeling for a given earthquake magnitude, but different realization of the initial conditions, gives similar values for both far-field zones and near-field ones.

7. CONCLUSION

The paper considers a catastrophic earthquake with a magnitude of $M = 8.1$, which occurred in the southern region of Mexico on September 8, 2017. Numerical simulation of the generation of tsunami waves by a seismic source and their propagation over the water area was carried out. Modeling was carried out for two different mechanisms of the seismic source, at different locations. A two-block and four-block source with a negative movement oriented towards the coast is considered. In the area of the 5-meter isobath, the distribution histograms for the maximum wave heights are plotted. Comparison of wave characteristics mareograms showed that the selected mechanisms of the seismic source give good agreement with the numerical values of both real data and a number of other authors. Figures 16-19 show that the above computations indicate a close distribution of the maximum wave heights along the Mexican coast. This indicates the correct tendency for the selection of the dynamics of the seismic source during the implementation of this earthquake.

Acknowledgments

REFERENCES

1. Mazova R.Kh. Soloviev S.L.. On influence of sign of leading tsunami wave on runup height on the coast // Science of Tsunami Hazards 12 (1994) 25-31.

2. M.RAMIREZ-HERRERA, N. CORONA, G. Suarez, A Review of Great Magnitude Earthquakes and Associated Tsunamis along the Guerrero, Mexico Pacific Coast: A Multiproxy Approach // American Geophysical Union. Published 2016 by John Wiley & Sons, Inc. 13 (2016)

3. R.WILSON, M. Ramirez-Herrera, L. Dengler, K. Miller, Y. LaDuke, Tsunami Generated by MW8.1 Chiapas, Mexico, Earthquake on September 7, 2017 // EERI Preliminary Notes on Tsunami Damage and Response , 13 (2017)

4. United States Geological Survey (USGS) https://earthquake.usgs.gov/

5. Pacific Coastal and Marine Science Center https://walrus.wr.usgs.gov/

6. Lobkovsky L.I. Geodynamics of spreading and subduction zones and two-level plate dynamics (Nauka Press, Moscow, USSR, 1988)

7. Voltzinger N. E., Klevanny K. A., Pelinovsky E. N. Long wave dynamics of the coastal zone, Leningrad: Gidrometeoizdat, 1989.272 p.

8. Pelinovsky E. N. Nonlinear dynamics of tsunami waves // Gorky: IAP USSR Acad.of Sci., 1982 .—226p.

9. Lobkovsky L.I., Mazova R.Kh., Baranov B.V., Kataeva L.Yu. Generation and propagation of tsunamis in the Sea of Okhotsk: possible scenarios // DAN, T.410, pp.528-532, 2006.

10. Lobkovsky L., Mazova R., Tyuntyaev S., Remizov I. Features and Pronlems with Historical Great Earthquakes and tsunamis in the Mediterranean Sea // Journal Science of Tsunami Hazards, Vol. 35, .No. 3, pp. 167-188, (2016).

11. Lobkovsky L., Garagash I., Baranov B., Mazova R., Baranova N., Modeling Features of Both the Rupture Process and the Local Tsunami Wave Field from the 2011 Tohoku Earthquake, Pure Appl. Geophys. (2017). V.174, p. 3919-3938, doi: 10.1007 / s00024-017-1539-5 (March 2017) pp.1-20.

12. WELLS D.L., Coppersmith K.J. New empirical relationships among magnitude, rupture length, rupture width, rupture area, and surface displacement // Bull. Seism. Soc. Am. 1994. Vol. 84. P. 974-1002

13. B. ADRIANO, E. Mas, S. Koshimura, Preliminary Tsunami Simulation of the Mw = 8.1 (USGS) - 96km SW of Pijijiapan, Mexico (ver. 2) // Laboratory of Remote Sensing and Geoinformatics for Disaster Management IRIDeS, Tohoku University, JAPAN, 7 (2017)

14. B. ADRIANO, Y. Fujii, S. Koshimura, E. Mas, A. Ruiz-Angulo, M. Estrada, Tsunami Source Inversion Using Tide Gauge and DART Tsunami Waveforms of the 2017 Mw8.2 Mexico Earthquake // Pure Appl ... Geophys. 175 (2018), 35–48

15. Global Disaster Alert and Coordination System (GDACS) http://www.gdacs.org/

16. Tsunami Bulletin Board, Tsunami Information Center (ITIC) http://www.ioc-sealevelmonitoring.org/